J|A|C|S COMMUNICATIONS

Published on Web 04/16/2009

Study of SERS Chemical Enhancement Factors Using Buffer Layer Assisted Growth of Metal Nanoparticles on Self-Assembled Monolayers

Masato M. Maitani,[†] Douglas A. A. Ohlberg,[§] Zhiyong Li,[*,§] David L. Allara,[*,†,‡] Duncan R. Stewart,[§] and R. Stanley Williams[§]

Department of Materials Science and Engineering, The Pennsylvania State University, University Park, Pennsylvania 16802, Department of Chemistry, The Pennsylvania State University, University Park, Pennsylvania 16802, and Information & Quantum Systems Laboratory, Hewlett-Packard Laboratories, 1501 Page Mill Road, MS1123, Palo Alto, California 94304

Received November 30, 2008; E-mail: dla3@psu.edu; zhiyong.li@hp.com

Surface enhanced Raman spectroscopy (SERS), with reported ultimate sensitivities of single molecule detection, is of great interest for sensor applications.[1] Both electromagnetic and chemical enhancements (EME, CE) contribute to SERS intensities, but much more work has focused on the former mechanism.[2] While the CE effect has been the subject of ongoing theoretical and experimental study for decades,[2−5] large disparities remain in reported CE factors (CEFs), ranging from ∼10 to 10^7, [2,4] often explained by sample preparation inconsistencies and lack of reliable experimental models or reference systems. Some early estimates of CEFs depended upon a precise theoretical calculation of the pure EME factors (EMEFs) based on the physical structure and electronic properties of the metal support with the estimated CEFs obtained by differences between predicted and observed SERS intensities.[5] To date no reliable, general experimental strategy appears to have been developed to isolate and quantitate these effects. Achieving accurate measurements would provide a valuable basis for accurate interpretation of SERS sensor data for varying analytes.

Here, we demonstrate a self-consistent experimental strategy to construct sets of samples with precisely known molecular coverages of molecules assembled within each SERS active structure and with identical EMEFs across the set, thereby allowing relative CEFs to be extracted. The strategy involves Au vapor deposition onto well-defined, chemically varied self-assembled monolayers (SAMs) via condensed inert gas buffer layer assisted growth (BLAG). The key idea is that BLAG conditions decouple the evolving Au nanoparticle (Np) film morphology from the SAM surface chemistry,[6] thereby forming pristine Np-SAM-Au sandwich films with uniform EMEFs. As a first demonstration, we show an example for two SAMs with chemically different terminal groups, $-CH_3$ and $-SH$, formed from 1,4-benzenedithiol (BDT) and 4-methylbenzenethiol (MBT) molecules assembled onto atomically flat template-stripped Au substrates (TS-Au),[7] as depicted in Figure 1.

The SAMs were assembled on fresh TS-Au substrates immersed in ethanol solutions of BDT and MBT under ambient N_2 and then systematically characterized by ellipsometry, infrared spectroscopy, tapping mode AFM, X-ray photoelectron spectroscopy, and surface plasmon resonance spectroscopy (SPRS) (see Supporting Information (SI) for details). The characterization results indicate that both SAMs have a well-organized, densely packed structure with the free $-SH$ and $-CH_3$ groups residing at the exposed film/ambient interface. The AuNp depositions were performed side by side on both SAMs under UHV conditions (base pressure: $\sim 5 \times 10^{-10}$ Torr)

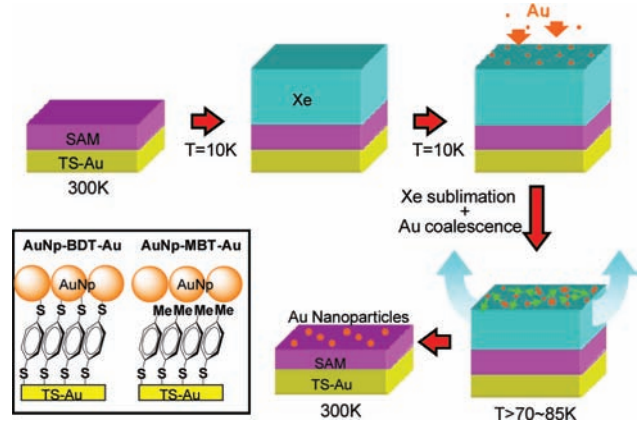

Figure 1. Schematics of BLAG AuNp deposition on SAMs.

to ensure uniformity across the two sample surfaces. The clean SAMs were mounted via a loadlock onto a manipulator cooled to ∼10 K prior to the Xe dosing. The condensed Xe layer thickness on the SAM was controlled by the dose exposure at a Xe pressure of 2×10^{-6} Torr.[7] Au vapor overlayer deposition was then performed by thermal evaporation (deposition rate: 1 Å·min^{-1}, sample temperature: ∼10.5 K, and chamber pressure during deposition: $\sim 2 \times 10^{-9}$ Torr). Following deposition, the Xe buffer layer was removed by controlled, slow uniform sublimation at 70−85 K with the chamber pressure maintained below 2×10^{-6} Torr (finally reaching $\sim 1 \times 10^{-9}$ Torr). Finally the AuNp-SAM-Au samples were heated to room temperature and removed to the ambient laboratory environment for SERS measurement and characterization.

In Figure 2, AFM images along with representative line profiles of the AuNp-SAM-Au samples illustrate that while the nanoparticle morphology depends on the thickness of the Xe buffer layer, the underlying SAM films have no evident effect on morphology. The thinnest buffer layers produce fairly uniformly distributed nanoparticles (I), thicker layers result in irregular aggregates (II), and sequential cycles of deposition and sublimation lead to a broad size distribution (III), but for each BLAG condition the two SAMs behave the same. This is a powerful advantage of BLAG over conventional physical vapor deposition, for which nanocrystal growth kinetics are strongly affected by the metal/SAM surface chemistry and undesired, uncontrollable ancillary processes can occur, e.g., filament growth and metal diffusion into the film/substrate interlayer.[8] The similar AuNp morphologies ($D = \sim 5$ nm) for condition (I) on both SAMs are further confirmed by size analyses based on AFM and cross-sectional TEM images of a AuNp (see Figure S3-1, -2).

[†] Department of Materials Science and Engineering, The Pennsylvania State University.
[§] Hewlett-Packard Laboratories.
[‡] Department of Chemistry, The Pennsylvania State University.

10.1021/ja809347y CCC: $40.75

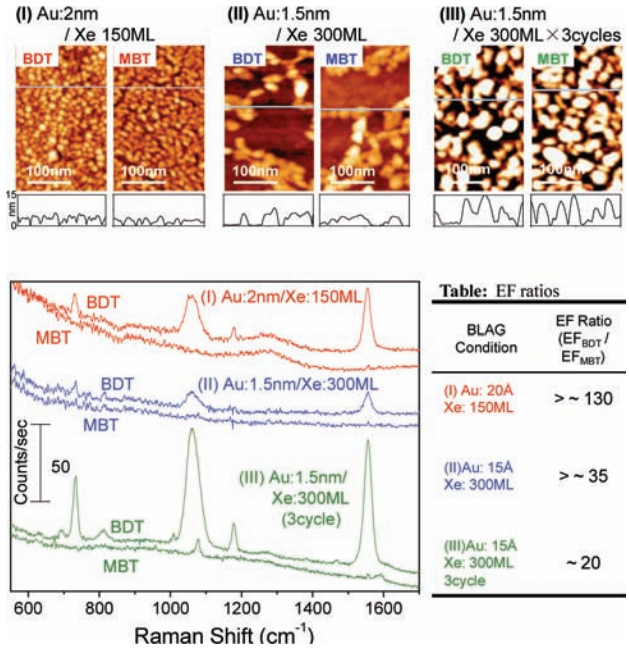

Figure 2. AFM images (0.4 μm × 0.2 μm) and corresponding SERS spectra (632.8 nm excitation) of AuNp-BDT-Au and AuNp-MBT-Au with BLAG conditions of (I) Au: 2 nm/Xe: 150 ML, (II) Au: 1.5 nm/Xe: 300 ML, and (III) [Au: 1.5 nm/Xe: 300 ML] × 3 cycles; Xe sublimation and Au deposition are defined as 1 cycle. EF ratio EF_{BDT}/EF_{MBT} is calculated for the 1557 cm^{-1} peak (mode 8a[9]) and summarized in the table.

The SERS vibrational spectra (Figure 2; assignments given in the SI) arise primarily from the SAM between the nanoparticle layer and the substrate, though we cannot completely rule out some contribution from stray molecules located in hot spots such as interparticle gaps. The latter appears to be minimal, however, based on control experiments in which 4-fluorobenzenethiol (FBT), a strong Raman scatterer, was postadsorbed onto both AuNp-BDT-Au and AuNp-MBT-Au samples prepared by BLAG conditions (I) and (III). In no case were FBT peaks observed (details given in the SI), whereas the MBT or BDT peaks remained. Control samples without AuNp overlayers exhibit no spectral features above the background noise, as expected because of the lack of a momentum matching condition for SPP excitation from an isolated planar surface (Figure S2-4). To establish suitability for quantitative analysis, measurements were made across the sample surface and over periods of time. For BDT samples prepared under BLAG condition (I), the SERS spectral intensity across the surface varies by ~5% within a sampling area of a few hundred μm^2 and ~10% within a sampled mm^2 region (Figure S5). Further, no spectral blinking or bleaching is observed for measurements over ~1 min (Figure S6). Thus the two criteria for reliable, quantitative analysis, spatial uniformity and temporal stability, are met.

Since the AuNp-BDT-Au and AuNp-BMT-Au systems are identical in all aspects except for the terminal functional groups, the difference in spectral intensities between their common vibrational modes can be attributed to the difference in the CEFs between the AuNps and the two SAM systems. Values of the CEF_{BDT}/CEF_{MBT} ratios were determined from integrated intensities of the 1557 cm^{-1} peak and are summarized in the table in Figure 2. Depending on the BLAG conditions, the ratio varies from 20 to 130. Since no resolvable MBT SERS peaks for conditions (I) and (II) are observed above the baseline noise, integrated intensities represent upper limits; accordingly the corresponding CEFs represent lower limits. The observation that BDT, which can form strong S−Au bonds with the AuNps, always shows significantly higher spectral intensity than MBT, where there are no such bonds, is consistent with the general trend of CE, where strong chemical interactions between a metal surface and a molecule increase the enhancement of SERS.[2,4] Since the uniformity of the AuNp layer was much better for condition (I), we assign the most reliable CEF ratio to be ~130.

In summary, we have demonstrated that AuNp-SAM-Au structures fabricated by Au vapor deposition onto SAMs with a cryogenically cooled, top Xe buffer layer provide a clean, simple platform to study the CE factor of SERS. Structures with a BDT SAM show an SERS enhancement factor ~130 times more intense than that for an MBT SAM. The key factor underlying this difference is the presence of the strong chemical bond between the top thiol and the AuNp in the BDT SAM. The important advantages of this experimental strategy for isolating SERS CE effects are the use of pristine AuNp/SAM interfaces, uncomplicated by surfactant shells that typically encapsulate metal nanoparticles, metal morphologies that are highly independent of the SAM surface chemistry, and the ability to vary the chemical character of the AuNp/SAM interface via SAM terminal groups and structural systems. To elucidate the exact mechanistic details of the intensity differences between BDT and MBT, theoretical modeling and experiments with other species of SAMs and metals are in progress for future reports.

Acknowledgment. We thank Josh Maier, Thomas Daniel for materials characterization (PSU), Jianhua Yang, Pamela Long, and Xuema Li for sample preparations (HP Laboratories), John Wendelken and An-Ping Li (ORNL) for assistance in BLAG chamber design. This work is partially supported by DARPA and DTRA.

Supporting Information Available: Full experimental details and characterizations This material is available free of charge via the Internet at http://pubs.acs.org.

References

(1) (a) Van Duyne, R. P.; Kneipp, K.; Kneipp, H.; Schatz, G. C. *Surface-Enhanced Raman Scattering - Physics and Applications*; Springer: Berlin/Heidelberg, 2006. (b) Kneipp, K.; Kneipp, H.; Itzkan, I.; Dasari, R. R.; Feld, M. S. *Chem. Rev.* **1999**, *99*, 2957–2976. (c) Kneipp, K.; Wang, Y.; Kneipp, H.; Perelman, L. T.; Itzkan, I.; Dasari, R. R.; Feld, M. S. *Phys. Rev. Lett.* **1997**, *78*, 1667–1670.

(2) (a) Van DuyneR. P. *Chemical and Biochemical Applications of Lasers*; Academic Press: New York, 1979; Vol. 4. (b) Moskovits, M. *Rev. Mod. Phys.* **1985**, *57*, 783. (c) Otto, A.; Mrozek, I.; Grabhorn, H.; Akemann, W. *J. Phys.: Condens. Matter* **1992**, *4*, 1143–1212.

(3) (a) Albrecht, A. C. *J. Chem. Phys.* **1961**, *34*, 1476–1484. (b) Lombardi, J. R.; Birke, R. L.; Lu, T.; Xu, J. *J. Chem. Phys.* **1986**, *84*, 4174–4180. (c) Arenas, J. F.; Woolley, M. S.; Tocon, I. L.; Otero, J. C.; Marcos, J. I. *J. Chem. Phys.* **2000**, *112*, 7669–7683.

(4) (a) Campion, A.; Kambhampati, P. *Chem. Soc. Rev.* **1998**, *27*, 241–250. (b) Fromm, D. P.; Sundaramurthy, A.; Kinkhabwala, A.; Schuck, P. J.; Kino, G. S.; Moerner, W. E. *J. Chem. Phys.* **2006**, *124*, 061101−061104. (c) Zhou, Q.; Fan, Q.; Zhuang, Y.; Li, Y.; Zhao, G.; Zheng, J. *J. Phys. Chem. B* **2006**, *110*, 12029–12033. (d) Tian, Z. Q.; Ren, B.; Wu, D. Y. *J. Phys. Chem. B* **2002**, *106*, 9463–9483. (e) Peyser-Capadona, L.; Zheng, J.; Gonzalez, J. I.; Lee, T. H.; Patel, S. A.; Dickson, R. M. *Phys. Rev. Lett.* **2005**, *94*, 058301−058304.

(5) Murray, C. A.; Bodoff, S. *Phys. Rev. B.* **1985**, *32*, 671–687.

(6) (a) Haley, C.; Weaver, J. H. *Surf. Sci.* **2002**, *518*, 243–250. (b) Waddill, G. D.; Vitomirov, I. M.; Aldao, C. M.; Weaver, J. H. *Phys. Rev. Lett.* **1989**, *62*, 1568–1571. (c) Waddill, G. D.; Vitomirov, I. M.; Aldao, C. M.; Anderson, S. G.; Capasso, C.; Weaver, J. H. *Phys. Rev. B* **1990**, *41*, 5293–5305. (d) Yoo, K.; Li, A.-P.; Zhang, Z.; Weitering, H. H.; Flack, F.; Lagally, M. G.; Wendelken, J. F. *Surf. Sci.* **2003**, *546*, L803−L807.

(7) Lee, S.; Bae, S. S.; Medeiros-Ribeiro, G.; Blackstock, J. J.; Kim, S.; Stewart, D. R.; Ragan, R. *Langmuir* **2008**, *24*, 5984–5987.

(8) Herdt, G. C.; Jung, D. R.; Czanderna, A. W. *Prog. Surf. Sci.* **1995**, *50*, 103–129.

(9) (a) Varsanyi, G. *Assignments for Vibrational Spectra of Seven Hundred Benzene Derivatives*; John Wiley & Sons: New York, 1974. (b) Cho, S. H.; Han, H. S.; Jang, D. J.; Kim, K.; Kim, M. S. *J. Phys. Chem.* **1995**, *99*, 10594–10599. (c) Weckenmann, U.; Mittler, S.; Naumann, K.; Fischer, R. A. *Langmuir* **2002**, *18*, 5479–5486.

JA809347Y